Assignment of Asparagine-44 Side-Chain Primary Amide ^{1}H NMR Resonances and the Peptide Amide N^{1}H Resonance of Glycine-37 in Basic Pancreatic Trypsin Inhibitor†

Erik Tüchsen* and Clare Woodward‡

Department of Chemistry and Biology, Roskilde University, DK4000, Roskilde, Denmark, and Department of Biochemistry, University of Minnesota, St. Paul, Minnesota 55108

Received July 29, 1986; Revised Manuscript Received November 12, 1986

ABSTRACT: New assignments of three previously undetected amide proton NMR resonance lines in bovine pancreatic trypsin inhibitor are reported. These are the peptide amide proton of Gly-37 and the primary amide protons of Asn-44. Specific assignments of Asn-44 and Asn-43 H_E and H_Z resonances are also reported. The Gly-37 NH and Asn-44 H_Z resonances are shifted upfield to 4.3 and 3.4 ppm, respectively, by the ring current of the Tyr-35 aromatic group, while Asn-44 H_E resonates at 7.8 ppm. The abnormal chemical shifts of Asn-44 H_Z and Gly-37 NH indicate that both NH's interact with the π-electron cloud of the Tyr-35 ring. This is consistent with their location in the crystal structure. The resonances are resolved by differential labeling techniques and are studied by combined use of NOE and exchange difference spectroscopy.

Exchange of labile peptide protons is widely used to assess protein dynamics. Protons of the primary amide groups in Asn and Gln residues are used much less frequently for this purpose. In hydrogen-exchange studies the side-chain primary amide protons have often been disregarded as too rapidly exchanging to contribute to the observed kinetics because their chemical exchange rate is higher than for peptide protons and because many are exposed to the solvent on the surface of the protein. However, it is expected that buried primary amide protons will exchange slower than model amides (Ottesen, 1972; Richarz et al., 1979) and that their exchange kinetics will also reflect the dynamic structure of folded proteins. We have therefore undertaken a study of these in BPTI.[1]

In BPTI there are two buried primary amide groups, the side chains of Asn-43 and Asn-44. Their local environments in the crystal structure are interesting. The Asn-43 primary amide group makes three H bonds with peptide backbone groups, as shown in Figure 1a. The carbonyl O is an H-bond acceptor from Tyr-23 peptide NH, H_Z is an H-bond donor to Tyr-23 carbonyl O, and H_E is a donor to Glu-7 carbonyl O. The peptide NH's of Tyr-21, Phe-22, and Tyr-23 are the slowest exchanging in BPTI (Simon et al., 1984), and the exchange rate of the Asn-43 side chain is comparable.

The Asn-44 NH_2 adjoins a cavity containing three internal water molecules, Wat-111, Wat-112, and Wat-113. As shown in Figure 1b, Asn-44 side-chain carbonyl O is an H-bond acceptor for the guanidino group of Arg-20 and H_E makes an H bond with the oxygen of Wat-113. H_Z faces the aromatic ring of Tyr-35, very close to the center of the ring. Symmetrically located on the other side of the Tyr-35 ring is the peptide NH of Gly-37, also oriented toward the center of the ring. Both Asn-44 H_Z and Gly-37 NH are in close contact with the π-electron cloud of Tyr-35 and appear to be examples of polar interactions with aromatic groups suggested by Wlodawer et al. (1984) and by Perutz et al. (1986) and investigated by Burley and Petsko (1986).

Neither the Asn-44 protons nor the Gly-37 peptide NH has been assigned in the ^{1}H NMR spectrum. We report here new assignments of the two Asn-44 N$^\delta$H's and the peptide NH of Gly-37 and specific assignments of Asn-43 and Asn-44 H_Z and H_E. These complete the total assignment of all primary and secondary amide protons in BPTI.

Methods

The use of ^{1}H labeling procedures to sort out specific groups of exchangeable proton resonances in the NMR spectrum has been extensively used and is described in detail elsewhere (Tüchsen & Woodward, 1985, 1987a,b). Samples described in the present paper contain 1.5–3 mM BPTI (Aprotinin, Novo; Novo Industries, Copenhagen, batch 32-65 or B3007-86) and 0.3 M KCl. Values of pH are direct pH meter readings calibrated by standard commercial buffers in natural water.

The primary amide protons of Asn-43 were studied in samples prepared by dissolving fresh BPTI in ^2H_2O at pH 8.6. At this pH most overlapping ^{1}H NMR resonances rapidly disappear, and the Asn-43 side-chain protons are observed along with resonances of the very stable β-core protons. Measurements at other pHs are made after incubation of the protein at pH 8.6 for 15–30 min and then adjustment to the experimental pH. This procedure was used for spectra in Figures 4b, 7, and 8.

Samples for Gly-37 NH (Figures 5 and 6) were prepared by dissolving fresh BPTI in ^2H_2O at pH 6.5 and then adjusting to the experimental pH.

The Asn-44 N$^\delta$H resonances are resolved by a specific ^{1}H labeling procedure that takes advantage of the high pH_{min} of primary amide protons (Tüchsen & Woodward, 1987a). First, the protein is deuteriated at all exchangeable sites by heating

† Supported by NIH Grant 26242 and a grant from the Danish Natural Sciences Research Council.

* Address correspondence to this author at Roskilde University.
‡ University of Minnesota.

[1] Abbreviations: BPTI, basic pancreatic trypsin inhibitor; NMR, nuclear magnetic resonance spectroscopy; ppm, parts per million; NOE, nuclear Overhauser enhancement; FID, free induction decay; COSY, two-dimensional *J*-correlated spectroscopy; NOESY, two-dimensional NOE-correlated spectroscopy.

0006-2960/87/0426-1918$01.50/0

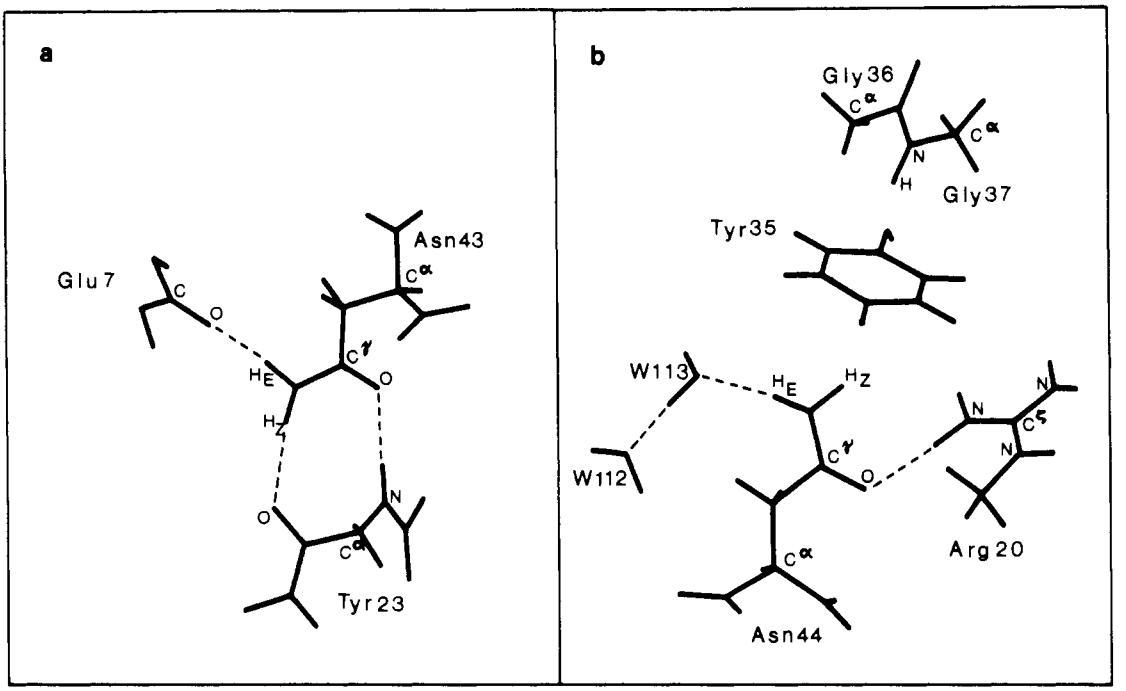

FIGURE 1: (a) Crystal structure configuration of the Asn-43 side chain. (b) Structure of BPTI in the surroundings of the Tyr-35 aromatic ring.

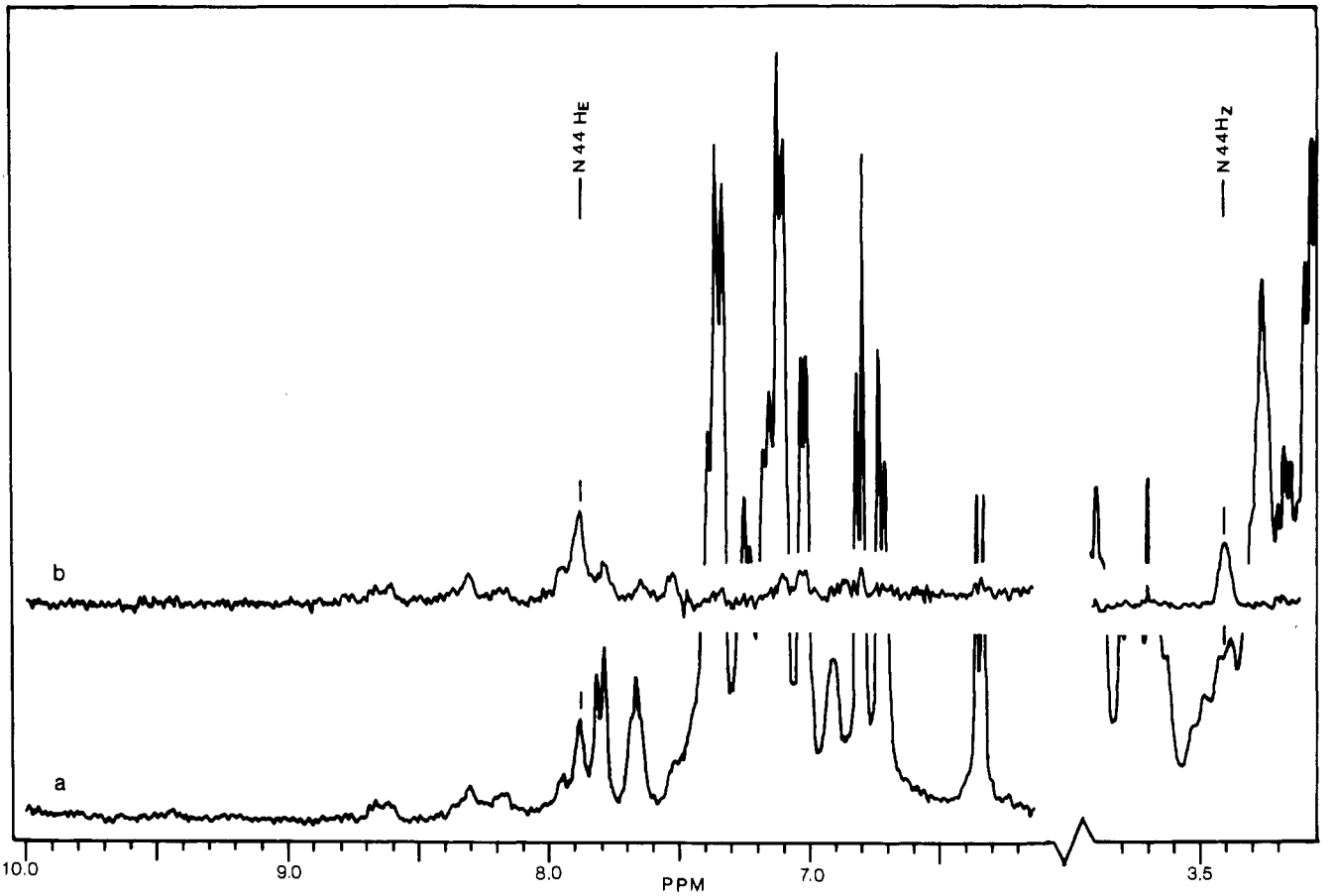

FIGURE 2: 300-MHz spectra at pH 5.7 of BPTI with specific ^1H label at Asn-44 $N^{\delta}H_2$. Spectrum a is the full spectrum. Spectrum b is an exchange difference spectrum obtained by subtracting a spectrum of the fully deuteriated protein from spectrum a. The scaling factor of spectrum a is reduced in the 3–4-ppm region. The sample (3 mM BPTI in 0.3 M KCl) was first fully labeled with ^2H, then in-exchanged with ^1H at pH 1.0 for 1 h, and subsequently reexchanged with ^2H at pH 4.6 for 2 h. For details see Methods.

to 90 °C in ^2H_2O. It is then freeze-dried, dissolved in natural water, and incubated for 1 h at pH 1.0, 25 °C. During this period the Asn-44 primary amide group exchanges to equilibrium, and along with it a number of secondary peptide amide groups obtain full or fractional ^1H label. These additional NH's are then reexchanged with ^2H by freeze-drying the sample, dissolving in ^2H_2O, and incubating at pH 4.6 for 1–2 h. The Asn-44 primary amide protons are the only NH's in the molecule that retain virtually full ^1H label. Spectra in Figures 2, 3, and 4b are of samples prepared in this way.

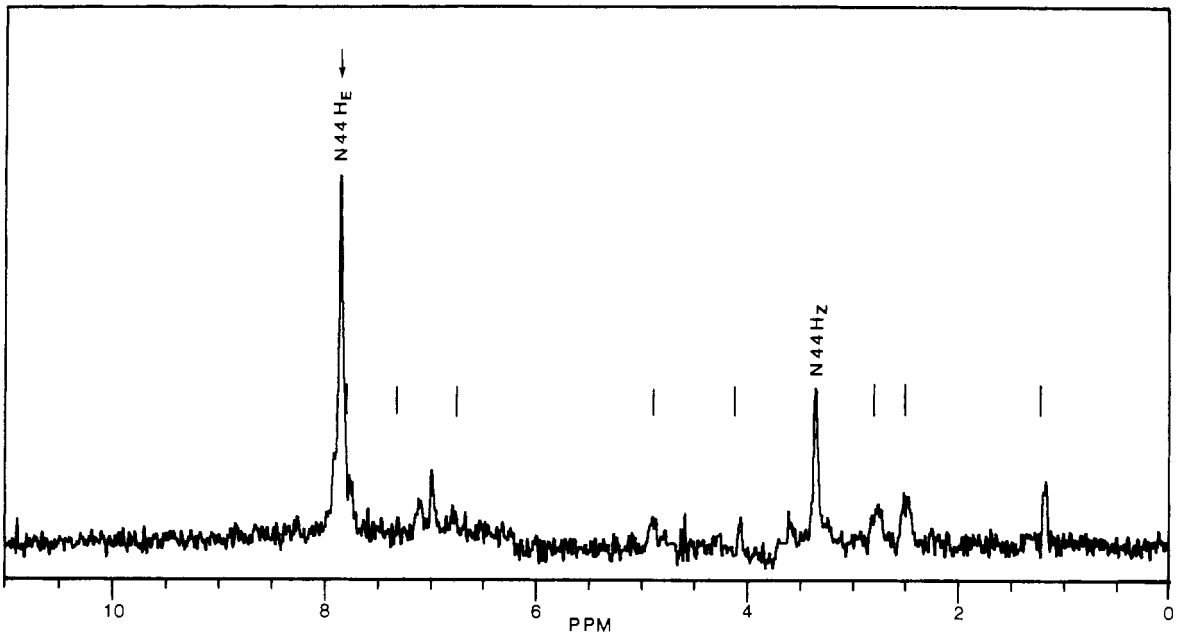

FIGURE 3: Exchange-NOE difference spectrum at 300 MHz, pH 6.2, obtained by irradiation of Asn-44 H_E at 7.8 ppm (arrow). The protein sample was specifically ^1H labeled at Asn-44 as described in the legend to Figure 2 and under Methods. NOE signals of overlapping nonexchangeable resonances are removed by subtracting an NOE difference spectrum measured after completion of the isotopic exchange. Vertical bars indicate literature chemical shifts of NOE's expected for Asn-44 H_E (cf. Table I). Noise signals at 4.7 and 3.6 ppm are zeroed.

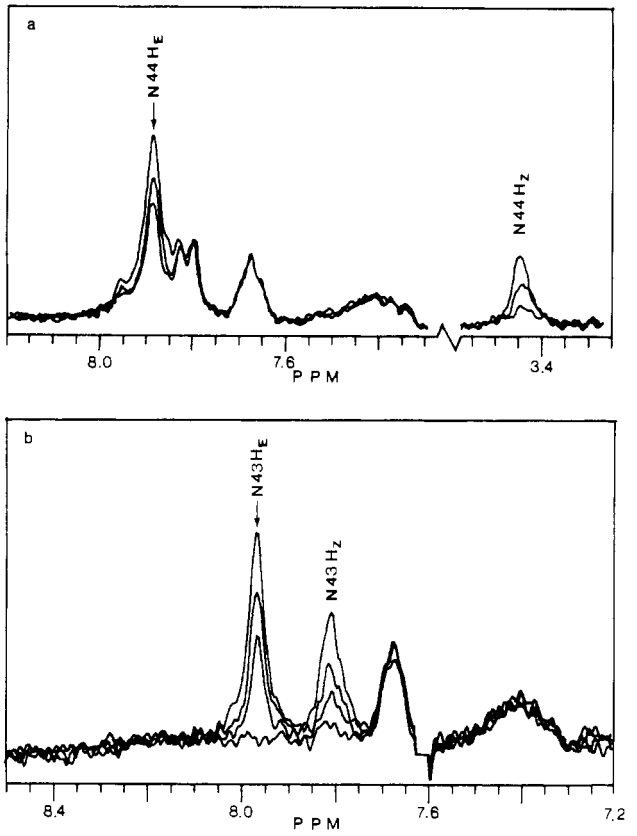

FIGURE 4: Stacked 300-MHz NOE difference spectra. (a) Asn-44 H_E (7.84 ppm) is saturated. Individual spectra represent 5-h time intervals at pH 6.1. (b) Asn-43 H_E (7.97 ppm) is saturated. Spectra were recorded at 2-h time intervals, pH 8.6. Samples in (a) and (b) were prepared for resolution of Asn-44 and Asn-43, respectively. Specific labeling of Asn-44 $N^\delta H$ for (a) is described in the legend to Figure 2 and under Methods. The sample for (b) is commercial BPTI dissolved in ^2H_2O (3 mM in 0.3 M KCl) and incubated at 25 °C for 30 min at pH 8.6. Arrows indicate the irradiation frequencies. A noise signal at 7.6 ppm in (b) is removed.

^1H NMR spectra were recorded at 300 (Nicolett 300 NMR), 500 (Bruker AM 500), or 250 MHz (Bruker AC 250). Regular proton NMR spectra were acquired in 4K or 8K data blocks by using a presaturation pulse sequence for saturation of the solvent signal. Freshly dissolved commercial protein contains a small amount of acetate, and the decoupler was used to saturate the signal from this impurity.

NOE difference spectra were obtained by an alternating scan method in which two FID's are collected simultaneously in adjacent blocks of memory. NOE's are generated in one spectrum by low-power continuous radio wave irradiation for 0.7 s at resonance frequency while in the other spectrum the frequency is shifted 10 ppm downfield outside the spectral region. The NOE's are observed in difference spectra obtained by subtracting the irradiated spectrum from the reference spectrum. 300-MHz NOE difference spectra were routinely collected in 2 × 4000 double precision data points, and each FID was summed of 5000–6000 transients. All spectra reported are at 25 °C.

The term "exchange difference spectra" is used for difference spectra obtained by subtracting spectra for a sample at different stages of exchange. Most often exchange difference spectra are obtained by subtracting a fully deuteriated spectrum from a given partially exchanged spectrum. Similarly, "exchange-NOE difference spectra" are exchange difference spectra between NOE difference spectra. These are useful in assignments of labile proton resonances. They contain only NOE's of labile protons while signals produced by spillover irradiation of nonexchangeable protons are subtracted.

Interatomic distances of H atoms in the BPTI crystal structure are taken from the coordinates of Wlodawer et al. (1984) for form II crystals. Because the structure was determined by joint refinement of neutron and X-ray diffraction data, it includes H atoms.

RESULTS

Asn-44 Side-Chain Amide Protons. Figure 2b shows an exchange difference spectrum of BPTI, partially labeled as described under Methods. For this, the spectrum of fully exchanged BPTI is subtracted from Figure 2a, the spectrum of partially labeled BPTI. The two exchangeable resonances in Figure 2b are specifically labeled by virtue of their high pH_{min} and their intermediate exchange rates, which are higher than for the β-core NH's and less than for the surface NH's.

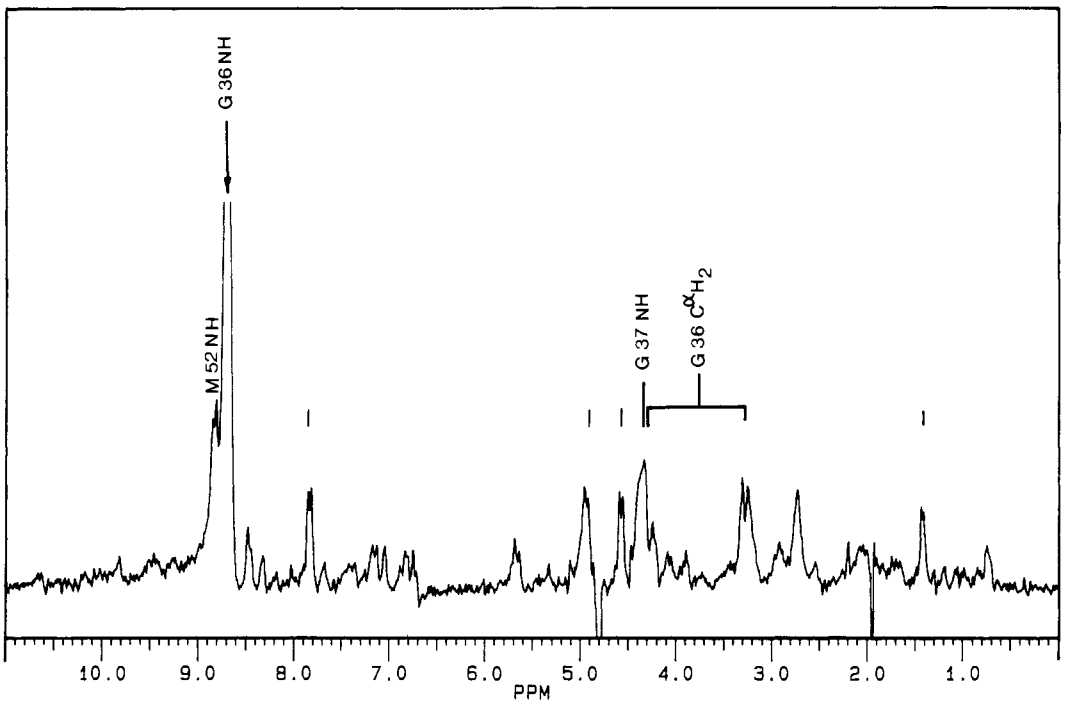

FIGURE 5: 250-MHz NOE difference spectrum showing NOE's from saturation of Gly-36 NH at 8.7 ppm (arrow). The sample contained 3 mM BPTI in ^2H_2O at pH 4.6. Resonances that overlap Gly-36 were removed by incubating the sample in ^2H_2O at pH 6.5 for 10 min. Vertical bars indicate expected NOE's from Gly-36 NH (cf. Table I).

Table I: Comparison of Observed NOE Chemical Shifts to Chemical Shifts of Protons in the Vicinity of Asn-44 H_E and Gly-37 NH

	distance[a] (Å)	chemical shifts (ppm) lit.	obsd NOE[b]
Irradiation at 7.86 ppm (Asn-44 H_E)			
Asn-44 $C^{\beta_1}H$	2.14	2.54[c]	2.50
Asn-44 $C^{\beta_2}H$	2.81	2.80[c]	2.74
Ala-40 $C^{\alpha}H$	3.02	4.13[c]	4.05
Ala-40 $C^{\beta}H_3$	2.73–4.17	1.23[c]	1.18
Asn-44 $C^{\alpha}H$	4.15	4.90[c]	4.93
Phe-33 $C^{\zeta}H$	2.71	7.33[c]	n.o.[e]
Tyr-35 $C^{\delta_1}H$	3.51	7.83[d]	7.76
Tyr-35 $C^{\epsilon_1}H$	3.92	6.75[d]	(6.78)
Irradiation at 8.66 ppm (Gly-36 NH)			
Gly-37 NH	2.78	n.o.	4.32
Gly-36 $C^{\alpha_1}H$	2.32	3.28[c]	3.26
Gly-36 $C^{\alpha_2}H$	2.80	4.33[c]	4.30
Tyr-35 $C^{\alpha}H$	2.44	4.90[c]	4.94
Thr-11 $C^{\alpha}H$	3.00	4.55[c]	4.56
Thr-11 $C^{\gamma}H_3$	2.58–3.08	1.40[c]	1.41
Tyr-35 $C^{\delta_1}H$	2.75	7.83[d]	7.81

[a] Calculated from the form II crystal structure coordinates of Wlodawer et al. (1984). [b] Taken from spectra in Figures 3 (Asn-44 H_E) and 5 (Gly-36 NH). [c] Wagner & Wüthrich, 1982. [d] Snyder et al., 1975. [e] Not observed.

Table II: Comparison of Predicted Ring Current Shifts and Observed Chemical Shifts of Protons near the Tyr-35 Ring

	chemical shift (ppm) obsd	chemical shift (ppm) model compn	ring current effect obsd	ring current effect predicted[a]
Gly-37 NH	4.3	8.6[b]	−4.3	−2.1
Asn-44 H_Z	3.4	6.9[c]	−3.5	−2.2
Asn-44 H_E	7.9	7.6[c]	+0.3	−0.7

[a] Johnson & Bovey, 1958. [b] Swenson & Koob, 1970. [c] Perrin et al., 1981.

The assignment of peaks at 7.9 and 3.4 ppm in Figure 2 to a primary amide group is made from the very strong mutual NOE observed in the exchange-NOE difference spectrum shown in Figure 3 and in the stacked NOE difference spectra in Figure 4a. NOE's of >50% are seen before the signal is decreased by isotope exchange. This very strong response of exchangeable protons in the NOE difference spectrum is expected only for two protons bound to the same N atom.

While assignment of the prominent peaks in Figure 2b to primary amide protons is based on the very strong NOE, assignment to Asn-44 can be made from the smaller NOE peaks in Figure 3. The exchange-NOE difference spectrum in Figure 3 facilitates analysis of the smaller NOE's because the NOE's produced by spillover to nonexchangeable protons have been subtracted. Irradiation in the 7.8–8.4-ppm region produces a large number of such NOE's in the aromatic and aliphatic regions, for example, Figure 4a. This is due to saturation of nonexchangeable aromatic protons (Phe-45 $C^{\epsilon}H$'s), which are broadened over this region by ring flipping. Additional unwanted NOE's are produced by the irradiation at 7.9 ppm by unavoidable spillover to the Tyr-35 $C^{\epsilon}H$ doublet at 7.8 ppm. All these irrelevant NOE's are eliminated by subtracting the NOE difference spectrum acquired after complete deuteriation of exchangeable hydrogens. The result in Figure 3 contains only NOE's originating from the exchangeable protons.

As listed in Table I, the observed NOE's in Figure 3 are in good agreement with the crystal structure for Asn-44 H_E. In the aliphatic region, 0–5 ppm, NOE's are observed for all H's within 4 Å of Asn-44 H_E at the chemical shifts, as listed by Wagner and Wüthrich (1982), and with intensities correlating well with calculated distances (Table I). The strongest NOE apart from that of the 3.4-ppm primary amide proton is at 1.2 ppm, a three-proton peak of Ala-40 $C^{\beta}H_3$. The distances between Asn-44 H_Z and the Ala-40 $C^{\beta}H$'s are 2.7–4.3 Å. The doublet-like appearance of the 1.2-ppm NOE supports this assignment. The broad NOE's at 2.5 and 2.7 ppm are from the Asn-44 $C^{\beta}H$'s at distances 2.14 and 2.81 Å, respectively. The NOE of Asn-44 $C^{\alpha}H$ at 4.93 ppm (Figure 3) is unusually intense for a distance of 4.15 Å.

The crystal structure contains three aromatic protons within 4 Å of Asn-44 H_E, Tyr-35 $C^{\delta_1}H$ at 3.51 Å, Tyr-35 $C^{\epsilon_1}H$ at 3.92 Å, and Phe-33 $C^{\zeta}H$ at 2.71 Å, respectively. Tyr-35 $C^{\delta_1}H$

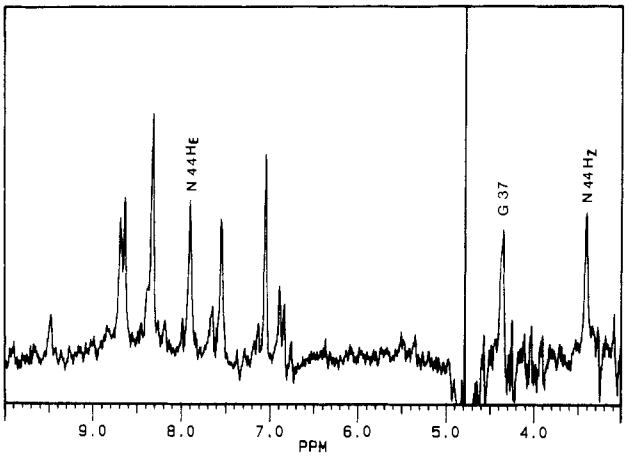

FIGURE 6: 500-MHz exchange difference spectrum. Two spectra were recorded 0.5 and 4.5 h after dissolving 3 mM BPTI in ^2H_2O at pH 7.1, and the difference spectrum was made by subtracting the last spectrum from the first. The vertical line at 4.8 ppm is due to uneven cancellation of the solvent signal.

is within the NOE distance of both Asn-44 H_E and Gly-36 NH (Figure 5). It is observed as a sharp doublet at 7.83 ppm in Figure 5 as well as in Figure 3 where it is partially overlapped with the irradiated peak. A very small peak at 6.8 ppm is compatible with the small NOE expected for Tyr-35 $C^{\epsilon 1}H$ at 6.75 ppm (Snyder et al., 1975). However, a strong NOE for Phe-33 $C^{\delta}H$ at 7.33 ppm (Wagner & Wüthrich, 1982) is not observed, and significant NOE's observed at 7.10 and 6.98 ppm are unaccounted for by the crystal structure. The latter are best matched by Phe-33 $C^{\delta}H_2$ and Phe-33 $C^{\epsilon}H_2$ listed at 7.13 and 7.20 ppm, respectively (Wagner & Wüthrich, 1982). Both of these are >4.1 Å away.

Specific assignment of the two Asn-44 primary amide protons to H_Z and H_E is obtained from the unusual chemical shift of the upfield resonance. In small primary amides the chemical shifts of H_E and H_Z are around 7.6 and 6.9 ppm, respectively (Perrin et al., 1981; Perrin & Johnston, 1981; Narutis & Kopple, 1983). In the crystal structure Asn-44 H_Z is very close to the ring of Tyr-35 and is centered approximately 2.6 Å over the ring plane, while H_E is about 4 Å away from the ring (Figure 1b). The large upfield shift for the 3.4-ppm resonance is explained by a ring current effect (Table II). The 3.4-ppm resonance is assigned to Asn-44 H_Z and the 7.9-ppm resonance to Asn-44 H_E.

Gly-37 Peptide Amide Proton. The resonance of Asn-44 H_Z at 3.4 ppm is the only upfield exchangeable resonance in partially labeled BPTI. However, similar spectra of BPTI with more extensive ^1H labeling show this resonance along with an additional exchangeable resonance at 4.3 ppm (Figure 6). For this spectrum BPTI is dissolved in ^2H_2O at pH 7.1 and spectra are accumulated 30 min and 4.5 h later. The 4.5-h spectrum is subtracted from the 30-min spectrum, and the resultant exchange difference spectrum contains resonances of NH's that exchange ^1H for ^2H over that period.

The labile proton resonance at 4.3 ppm is assigned to Gly-37 NH for several reasons. First, Gly-37 NH is the only remaining unassigned peptide proton in BPTI, so it is a likely candidate. Second, the large upfield shift similar to that of Asn-44 H_Z is expected because of the symmetric location of these two protons on either side of the Tyr-35 aromatic ring. Third, this assignment is in full agreement with the NOE's generated by saturation of Gly-36 NH at 8.66 ppm, given in Figure 5 and Table I.

In the NOE difference spectrum in Figure 5 a strong NOE of 20% is observed at 4.3 ppm, corresponding to the 4.3-ppm exchange difference peak in Figure 6. This strong NOE is predicted for the distance of 2.78 Å between Gly-36 NH and Gly-37 NH in the crystal structure. Significant NOE's are also observed for the Gly-36 $C^{\alpha}H$'s at 3.28 and 4.32 ppm, respectively, separated from Gly-36 NH by 2.8 and 2.3 Å, respectively. While the NOE at 3.28 ppm is a resolved doubletlike peak, only the upfield half of the 4.32-ppm doublet is resolved. The downfield half is overlapped with the resonance we assign to Gly-37 NH. Nevertheless, the resolution is sufficient to allow specific assignment of the two $C^{\alpha}H$'s based on relative NOE intensities and distances. The 3.28-ppm resonance is from the $C^{\alpha_2}H$ nearest to Gly-36 NH and the 4.32-ppm resonance is from $C^{\alpha_1}H$.

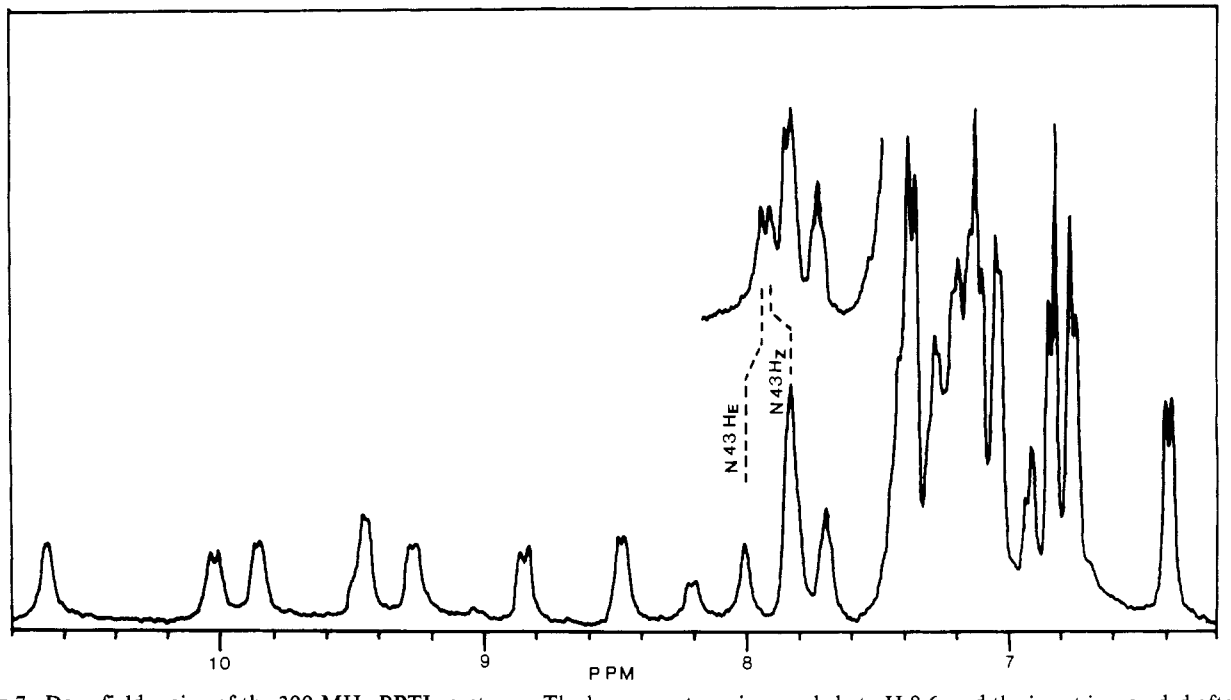

FIGURE 7: Downfield region of the 300-MHz BPTI spectrum. The lower spectrum is recorded at pH 8.6, and the insert is recorded after the sample is adjusted to pH 1.1. The sample preparation is as for Figure 4b.

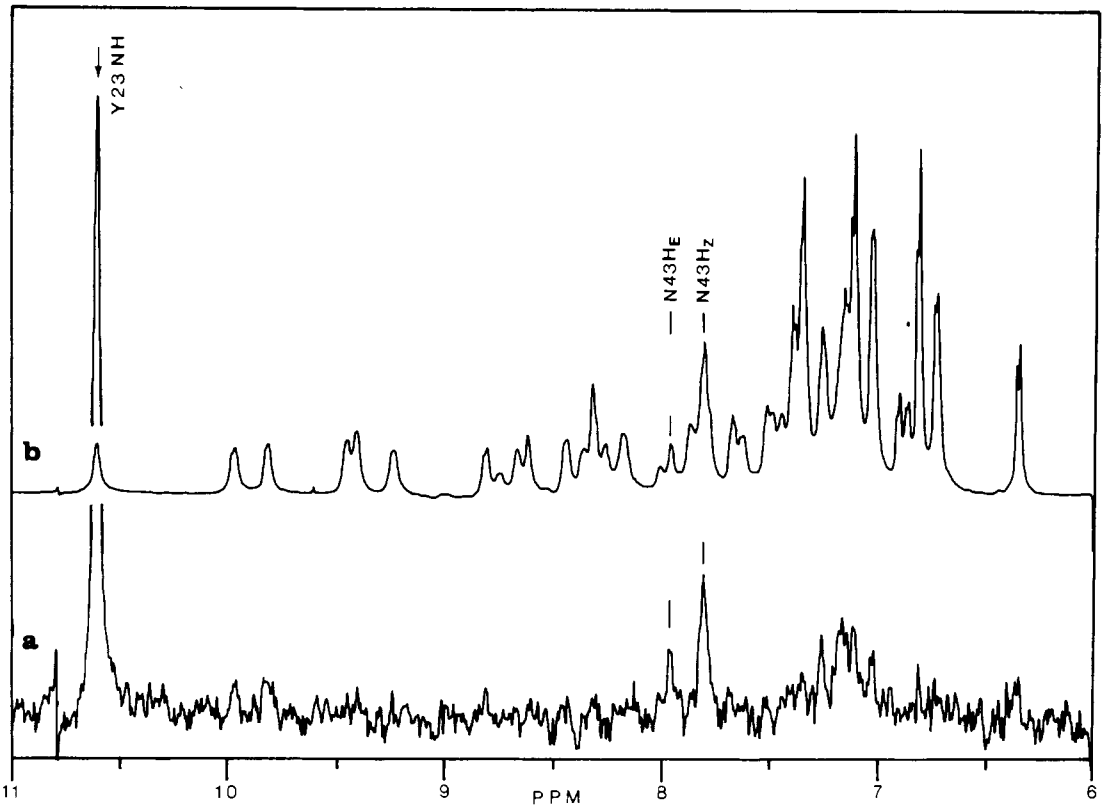

FIGURE 8: 500-MHz NOE difference experiment at pH 4.9: (a) NOE difference spectrum obtained by irradiating at the Tyr-23 NH resonance frequency, 10.6 ppm (arrow); (b) off-resonance irradiated spectrum. The sample preparation is as for Figure 4b.

Major NOE's are recognized in Figure 5 for all protons within 4 Å of Gly-36 NH at chemical shifts that correspond well with literature values. Also, many minor NOE's in Figure 5 are in agreement with the crystal structure and the literature assignments, e.g., the two $C^{\alpha}H$'s of Gly-37 at 2.9 and 4.2 ppm, respectively.

One major NOE at 2.70 ppm (Figure 5) is not accounted for by the protons in the vicinity of Gly-36 NH. The chemical shift and tripletlike shape suggest an assignment to Met-52 $C^{\gamma}H_2$, which may produce an NOE from spillover saturation of Met-52 NH. Met-52 NH, 8.84 ppm, is the partially overlapping downfield neighbor of Gly-36 NH in the NMR spectrum. The large NOE of ca. 30% for the 2.70-ppm resonance is interesting because it suggests a distance of less than 2.5 Å between Met-52 NH and $C^{\gamma}H_2$. In the form II crystal structure there are two alternative conformations of the Met-52 side chain (Wlodawer et al., 1984). In the high-occupancy conformation the distance between Met-52 NH and C^{γ} is 3.02 Å while in the low-occupancy conformation the distance is 0.12 Å less. The data suggest that the low-occupancy crystal structure conformation is predominant under the solution conditions of the present experiments.

Asn-43 Side-Chain Amide Protons. Both Asn-43 $N^{\delta}H$'s have previously been assigned by Wagner and Wüthrich (1982) at 7.97 and 7.77 ppm, and exchange has been measured for the resolved downfield $N^{\delta}H$ at varying pH in salt-free solutions. These NH's are remarkably slowly exchanging and can be followed in experiments designed for measurement of the exchange of the slowest β-core peptide NH's. After dissolution of BPTI at pH 8–9 the singletlike $N^{\delta}H$ resonance at 7.97 ppm is resolved while the other $N^{\delta}H$ at 7.85 ppm is overlapped with the peptide NH of Asn-24 and with the nonexchangeable downfield Tyr-35 $C^{\epsilon}H$ doublet (Figure 7).

The strong mutual NOE between these peaks is demonstrated in Figure 4b, showing four NOE difference spectra of

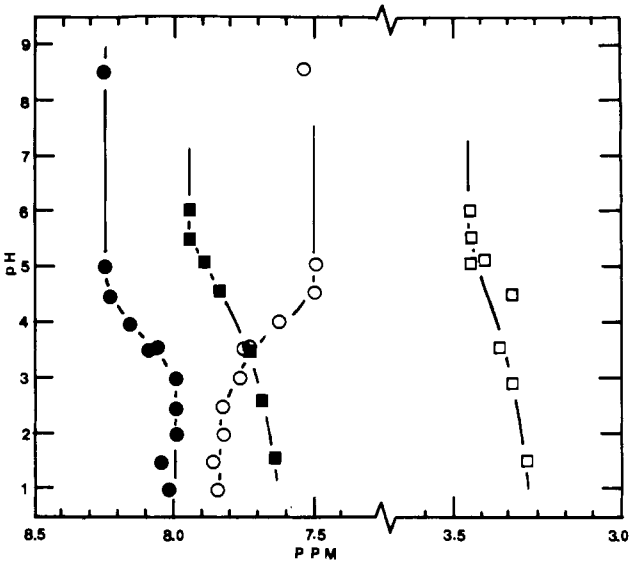

FIGURE 9: Chemical shift vs. pH for the buried primary amide protons: (●) Asn-43 H_E; (○) Asn-43 H_Z; (■) Asn-44 H_E; (□) Asn-44 H_Z.

a BPTI sample prepared as for Figure 7 (irradiation at 7.97 ppm). The four spectra are measured at 2, 6, and 8 h after dissolving in ^2H_2O and after completely deuteriating by heating at 90° for 10 min. During the experiment both peaks at 7.97 and 7.85 ppm gradually decrease, showing that they are of exchangeable resonances. The upfield peaks with unchanged intensity in Figure 4 arise from nonexchangeable protons. They are due to the saturation of the broadened Phe-45 $C^{\epsilon}H$, which produces a similarly broad NOE from the adjacent Phe-45 $C^{\delta}H$'s at 7.4 ppm and $C^{\zeta}H$ at 7.7 ppm.

Assignments of the two Asn-43 $N^{\delta}H$'s to H_E and H_Z, respectively, are made from the different NOE responses observed upon saturation of the nearby peptide NH of Tyr-23

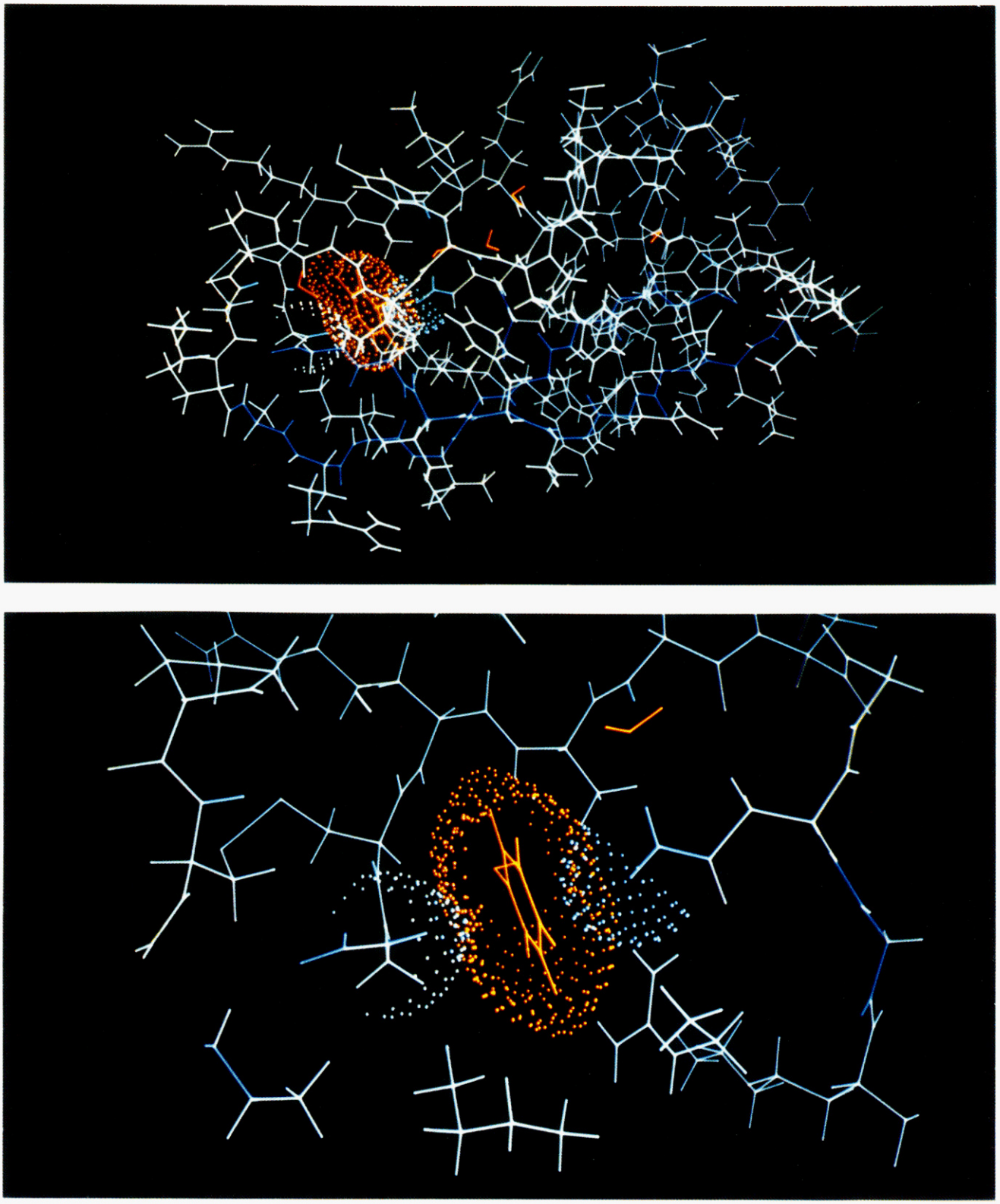

FIGURE 10: Gly-37 NH–Tyr-35 ring–Asn-44 H_Z network in BPTI. The crystal structure of form II BPTI, which includes the H atoms (Wlodawer et al., 1984), is shown. The van der Waals surfaces of Tyr-35 ring atoms (red), Gly-37 H (white), and Asn-44 H_Z (light blue) are highlighted. All these atoms are buried, except Tyr-35 OH. Heavy backbone atoms of the β-sheet, residues 16–36 and 44–45, are in dark blue in the lower portion of the molecule. Atoms of five buried water molecules [cf. Tüchsen and Woodward (1987b)] are in red. The full molecule is given at the top. The closeup section at the bottom is from the same orientation. The color pictures are obtained from the display of the program MIDAS at the University of California, San Francisco.

(10.6 ppm) (Figure 8). The distances in the crystal structure between Tyr-23 NH and Asn-43 H_E and H_Z are 4.0 and 2.7 Å, respectively, and therefore a much weaker NOE is expected for H_E than for H_Z. As seen in Figure 8 the weak NOE is observed for the downfield resonance, which is therefore assigned to H_E, while the upfield resonance at 7.77 ppm with the stronger NOE is assigned to H_Z. The overlap of the upfield resonance with the main-chain NH of Asn-24, the neighboring residue to Tyr-23, does not introduce any ambiguity in this assignment since the distance between Tyr-23 NH and Asn-24 NH in the crystal structure is 4.42 Å, and its contribution to the strong NOE at 7.77 ppm is small.

pH Dependence of Asn Chemical Shifts. The positions in the spectrum of the two Asn-44 side-chain NH's vary with pH (Figure 9). When the pH is lowered past the carboxyl titration region, both resonances move approximately 0.05 ppm upfield. The shape of the curve suggests that these resonances respond to two or more titrations with pK's separated by approximately 1 pH unit. In the crystal structure of BPTI distances between Asn-44 primary amide and the carboxyls of Glu-7 (pK = 3.9) and Asp-50 (pK = 3.2) are 9 and 12 Å, respectively. Similarly, both Asn-43 $N^{\delta}H$'s respond to a carboxyl titration. At pH <3.8 the two NH's move closer together, forming a doubletlike peak at 7.90–7.76 ppm (cf. insert of Figure 7). The symmetrical shape of the curve suggests that the titration is dominated by a single carboxyl with a pK about 3.8. The carboxylic side chain of Glu-7 is likely to be responsible for these shifts as one of the Asn-43 $N^{\delta}H$'s is hydrogen bonded to the main-chain carbonyl O of Glu-7 and the distance in the crystal structure between Asn-43 N^{δ} and the Glu-7 carboxylic group is 8 Å.

Discussion

BPTI contains 62 amide protons, 54 main-chain peptide protons, and 8 primary amide protons (1 Gln and 3 Asn). Although the ^1H NMR of BPTI has been extensively studied by several groups, the primary amide protons of Asn-44 and the peptide amide proton of Gly-37 have escaped detection. One reason for this is the unusual upfield shift of Gly-37 NH and Asn-44 H_Z resonances that places them midst the crowded methylene region of the spectrum. Further, the Gly-37 NH–$C^{\alpha}H$ cross-peaks are not easily located in the densely populated area close to the diagonal of COSY spectra, and it overlaps other cross-peaks in NOESY spectra. It seems doubtful that Gly-37 NH and Asn-44 H_Z would be located without the use of exchange difference spectra.

The unusual chemical shifts of Gly-37 NH and Asn-44 H_Z are partially explained by ring current magnetic deshielding. In the crystal structure they are located almost as mirror images on either side of the Tyr-35 aromatic ring (Figure 1). Theoretical calculations of ring current effects (Johnson & Bovey, 1958; Haigh & Mallion, 1972) were used by Perkins and Wüthrich (1979) to estimate ring current deshielding for a large number of protons facing the aromatic rings in BPTI. They concluded that the ring current effects determine the effect of protein tertiary structure on chemical shifts of aliphatic protons and that the Johnson–Bovey equation provides accurate estimates of these. For amide protons, in contrast, other effects contribute significantly, particularly hydrogen bonds to neighboring carbonyls.

In Table II, ring current effects taken from the original calibrated Johnson–Bovey diagram (Johnson & Bovey, 1958) are compared with the shifts observed for Asn-44 $N^{\delta}H_2$ and for Gly-37 NH. The Johnson–Bovey equation does predict large upfield shifts of >2 ppm for Gly-37 NH and Asn-44 H_Z and a smaller effect on Asn-44 H_E. However, the deshielding effects observed for Gly-37 NH and Asn-44 H_Z are about twofold larger than the effects calculated. The estimated upfield shifts for Gly-37 NH and Asn-44 H_Z of 2.1 and 2.2 ppm, respectively, are less than the observed effects of 4.3 and 3.5 ppm, respectively, and for H_E the estimated shift of −0.7 is of opposite sign compared with the observed +0.3 ppm. The discrepancy between ring current effects on CH's and NH's may be explained by their different chemical nature.

The identification of the Gly-37 resonance at 4.3 ppm is based on its isotope exchange, which is completed in a few hours at pH 7.1. There is an interesting discrepancy between this exchange rate and the very slow exchange of Gly-37 NH reported from neutron diffraction measurements of form II crystals by Wlodawer et al. (1984). In the crystals Gly-37 NH is apparently unexchanged after perfusion with ^2H_2O at pH 8.2 for 3 months. Other than Gly-37 NH, only the slowest β-core protons are unexchanged in the neutron diffraction experiment. This indicates a quenching of Gly-37 NH exchange rate of at least 3 orders of magnitude in the crystal as compared with solution.

Neither Gly-37 NH nor Asn-44 H_Z is within H-bonding distance to any of the usual protein or water acceptor atoms in the crystal structure. Also, both are well centered at 2.7–3.4 Å to all six-ring C atoms. Because of its proximity to the Tyr-35 ring, Wlodawer et al. (1984) suggested that the slow exchange of Gly-37 NH is due to its interaction with the Tyr-35 ring, which serves as an acceptor of a quasi H bond. Recently, there are indications of a general class of weak polar interactions, probably electrostatic in origin, which exists between the $\delta(+)$ of side-chain NH groups and the $\delta(-)$ π-electron cloud of aromatic groups in proteins (Perutz et al., 1986; Burley & Petsko, 1986). The Gly-37 NH–Tyr-35 ring–Asn-44 H_Z system, shown in Figure 10, appears to be a particularly good example of this type of interaction and in addition provides the first example of an H-bond network involving interactions on both sides of an aromatic ring.

Acknowledgments

We thank Dr. Tom Blundell for access to the molecular graphics facilities of Birkbeck College, University of London, and Dr. Robert Langridge for access to molecular graphics facilities of the University of California at San Francisco.

Registry No. BPTI, 9087-70-1; Asn, 56-40-6; Gly, 70-47-3.

References

Burley, S. K., & Petsko, G. A. (1986) *FEBS Lett. 203*, 139–143.

Haigh, C. W., & Mallion, R. B. (1972) *Org Magn. Reson. 4*, 203–228.

Johnson, C. E., & Bovey, F. A. (1958) *J. Chem. Phys. 29*, 1012–1014.

Narutis, V. P., & Kopple, K. D. (1983) *Biochemistry 22*, 6233–6239.

Ottesen, M. (1972) *Methods Biochem. Anal. 20*, 135–168.

Perkins, S. J., & Wüthrich, K. (1979) *Biochim. Biophys. Acta 576*, 409–423.

Perrin, C. L., & Johnston, E. R. (1981) *J. Am. Chem. Soc. 103*, 4697–4703.

Perrin, C. L., Johnston, E. R., Lollo, C. P., & Kobrin, P. A. (1981) *J. Am. Chem. Soc. 103*, 4691–4696.

Perutz, M. F., Fermi, G., Abraham, D. J., Poyart, C., & Bursaux, E. (1986) *J. Am. Chem. Soc. 108*, 1064–1078.

Richarz, R., Sehr, P., Wagner, G., & Wüthrich, K. (1979) *J. Mol. Biol. 130*, 19–30.

Simon, I., Tüchsen, E., & Woodward, C. (1984) *Biochemistry 23*, 2064–2068.

Snyder, G., Rowman, R., Karplus, S., & Sykes, B. D. (1975) *Biochemistry 14*, 3765–3777.

Swenson, A. S., & Koob, L. (1970) *J. Phys. Chem. 74*, 3376–3380.

Tüchsen, E., & Woodward, C. (1985) *J. Mol. Biol. 185*, 405–419.

Tüchsen, E., & Woodward, C. (1987a) *J. Mol. Biol.* (in press).

Tüchsen, E., & Woodward, C. (1987b) *Biochemistry* (in press).

Wagner, G., & Wüthrich, K. (1982) *J. Mol. Biol. 155*, 347–366.

Wlodawer, A., Walter, J., Huber, R., & Sjölin, L. (1984) *J. Mol. Biol. 180*, 301–329.